Boundary force exerted on spatial solitons in cylindrical strongly nonlocal media

Qian Shou,[1] Yanbin Liang,[1] Qun Jiang,[1] Yajian Zheng,[1] Sheng Lan,[1] Wei Hu,[1,2] and Qi Guo[1,3]

[1]*Laboratory of Photonic Information Technology, South China Normal University, Guangzhou 510631, China*
[2] *huwei@scnu.edu.cn*
[3] *guoq@scnu.edu.cn*

Received July 16, 2009; revised September 20, 2009; accepted September 24, 2009;
posted October 13, 2009 (Doc. ID 114207); published November 11, 2009

We investigate the propagation of spatial solitons in cylindrical strongly nonlocal media by a method of image beam of light. The dynamic force of the soliton steering resulting from the boundary effect is equivalent to the force between the soliton beam and the image beam. The trajectory of the soliton is analytically studied, which is in good agreement with the experimental results. © 2009 Optical Society of America

OCIS codes: 190.5940, 190.6135, 190.4870.

Nonlocal spatial solitons have been extensively investigated [1–16] since the pioneering work of Snyder and Mithchell [1]. A topic that has captured a rising interest is the interaction between solitons and boundaries [4–8], especially in lead glass. The group of Morderchai Segev found the boundary caused elliptic solitons and vortex solitons in lead glass and discussed the influence of the boundary force on the soliton trajectory [5,6]. In liquid crystal, Alberucci *et al.* demonstrated the power-depended soliton repulsion at the boundary [7,8]. The nonlocal nature of lead glass lies in the thermal optical nonlinearity (Poisson type), which is intrinsically infinite without boundaries [5]. Therefore, the behavior of the nonlocal solitons in lead glass can be greatly influenced by the remote boundary and one can obtain the soliton steering controlled by the asymmetric boundary force [6]. The long-range action of the boundary on the soliton compared with the soliton width suggests that the problem of the soliton trajectory can be settled by the method of the equivalent particle theory and the light ray equation [6,17], and the soliton can be taken as a point light in the cross section of the propagation medium.

In this Letter by analogy with the method of images in the electrostatics, we introduce a method of image beam of light to deal with the problem of the boundary effect on the soliton trajectory in cylindrical lead glass. The boundary force exerted on the soliton can be equivalent to the force of a remote image beam of light on the soliton. The experimental data of the soliton steering can be fitted by the analytical solution in good agreement.

The system we concern is the light-induced thermal self-focusing nonlinearity in lead glass. Optical energy is weakly absorbed with an absorption coefficient α and diffused with a thermal conductivity κ. The cylindrical boundary of the lead glass is thermally contacted by a copper-made heat sink at a fixed temperature T_0 described by Fig. 1(a). A temperature gradient is yielded whose distribution is governed by the Poisson equation [5]

$$\nabla^2 T(X,Y) = -\frac{\alpha}{\kappa} I(X,Y),$$

$$T(X,Y)|_{X^2+Y^2=R^2} = T_0, \tag{1}$$

where $T(X,Y)$ is the temperature distribution, $I(X,Y)=|A(X,Y)|^2$ is the light intensity with $A(X,Y)$ being the paraxial beam, and R is the radius of the cylinder. The heat transfer equation is inherently two-dimensional with a circular boundary as the soliton is invariant in the direction of propagation. The laser-induced temperature change $\Delta T=T-T_0$ gives rise to a proportional increase in the refractive index [5] $\Delta n=\beta\Delta T$, with β being the thermo-optical coefficient. In reverse, the refractive index change has a strong impact on the propagation characteristics of the light beam, including the focusing and the steering. The propagation of an optical beam in lead glass is modeled by Eq. (1) coupled with the equation for the paraxial beam $A(X,Y)$

$$\nabla^2 A + 2ik\frac{\partial A}{\partial z} + 2k^2\frac{\Delta n}{n_0}A = 0, \tag{2}$$

where $k=\omega n_0/c$, n_0 being the linear refractive index of the medium. We rewrite Eqs. (1) and (2) in a dimensionless form:

$$i\partial_z\varphi + \frac{1}{2}\nabla_\perp^2\varphi + N\varphi = 0, \tag{3a}$$

$$\nabla_\perp^2 N(x,y) = -|\varphi|^2, \tag{3b}$$

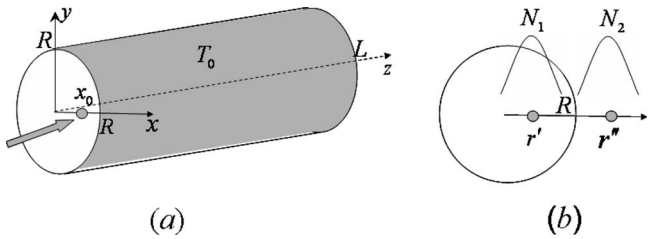

Fig. 1. (a) Diagrammatic layout of a soliton launched at an offset of x_0 in a circular cross section of the sample with radius R. (b) Sketch map of the normalized refractive indexes respectively induced by the soliton beam and the image beam.

0146-9592/09/223523-3/$15.00

$$N(x,y)|_{x^2+y^2=1} = 0, \tag{3c}$$

where $x=X/R$, $y=Y/R$, and $z=Z/(kR^2)$ are normalized coordinates; $\varphi=A/A_0$, with $A_0^2=n_0\kappa/(\alpha\beta k^2R^2)$; and $N=k^2R^2\Delta n/n_0$. It is noticeable that N and $|\varphi|^2$ in Eq. (3b) have their counterparts in the electrostatics, potential, and charge density, respectively.

We solve the light-induced refractive index distribution in the view of the Green's function method. In circular domain, the Green's function of Poisson equation can be deduced by the method of images [18], which is the sum potential of the source charge and the image charge

$$G = \frac{1}{2\pi}\left(\ln\frac{1}{|\mathbf{r}-\mathbf{r}'|} - \ln\frac{r''}{|\mathbf{r}-\mathbf{r}''|}\right) = G_1 + G_2, \tag{4}$$

where $\mathbf{r}(x,y)$, $\mathbf{r}'(x',y')$, and $\mathbf{r}''(x'',y'')$ are, respectively, the normalized radius vectors of the field point, the source point, and the image point, and $r''=1/r'$ described in Fig. 1(b). The image charge simulates the influence of all the inductive charges on the boundary, so the force applied to the source charge by the boundary is equivalent to the force between the image charge and the source charge. In our present case, when the source beam of light has a beam width small enough compared with the boundary size, it can be taken as a point beam of light. Borrowing ideas from the method of images in the electrostatics we introduce the method of image beam of light. By analogy with the expression of the charge interaction, we directly write the "force" between the source and image beams, which provides the dynamic force for the steering of the source beam,

$$f = \frac{\mathrm{d}^2x_c}{\mathrm{d}z^2} \propto \frac{p}{1/x_c - x_c}, \tag{5}$$

where $(x_c,0)$ is the center of the source beam and $(1/x_c,0)$ is the center of the image beam. y has been set zero, since the problem is y symmetric. $p=\int|\varphi(x'-x_c,y')|^2\mathrm{d}x'\mathrm{d}y'$ is the normalized light power, which is equivalent to the charges in the electrostatics. The $1/r$ law of interaction is ever predicted by Rostschild *et al.* [3]. It is notable that the force between the soliton to its image can be only attraction force, since the power cannot have negative values, in contrast to the electric charge.

The interaction of the two beams is mediated by the light-induced refractive index, which is the solution of Eq. (3b). When we make further quantitative analysis, the solution is given by

$$N = \int (G_1+G_2)|\varphi(x'-x_c,y')|^2\mathrm{d}x'\mathrm{d}y' = N_1 + N_2. \tag{6}$$

The integration has been expressed in two terms of N_1 and N_2. N_1 is symmetric about the beam center $(x_c,0)$, since G_1 is shift invariant and the beam has a symmetric profile (in the general case). It represents the source beam induced refractive index in the free space, which inversely serves as the focusing lens for the source beam to form solitons. For an incident beam with the given width w_0, we can obtain the critical power of the soliton $P_c=4\pi n_0\kappa/(\alpha\beta k^2w_0^2)$ by expanding N_1 to the second order [19]. The effect of N_2 on the source beam is equivalent to the effect of the refractive index induced by the image beam located at the image point $(1/x_c,0)$ indicated in Fig. 1(b).

In the case of $w_0 \ll R$, G_2 is almost unchanged in the profile of the light beam, N_2 reads

$$N_2 = -\frac{1}{2\pi}\int \ln\frac{r''}{|r-r''|}|\varphi(x'-x_c,y')|^2\mathrm{d}x'\mathrm{d}y' = -\frac{p}{2\pi}\ln\frac{1/x_c}{\sqrt{(x-1/x_c)^2+y^2}}. \tag{7}$$

The steering trajectory of a light ray is governed by the Eikonal equation [9,17]

$$\frac{\mathrm{d}^2x_c}{\mathrm{d}z^2} = \left.\frac{\mathrm{d}N_2}{\mathrm{d}x}\right|_{x=x_c,y=0} = -\frac{p}{2\pi}\frac{1}{1/x_c - x_c}. \tag{8}$$

Just as our qualitative anticipation in Eq. (5), the acceleration of the source beam center has a form analogous to that of the interforce between the source and the image charges. We expand the right-hand side of Eq. (8) with respect to x_c about $x_c=0$ under the condition of $x_c \ll 1$,

$$\frac{\mathrm{d}^2x_c}{\mathrm{d}z^2} = -\frac{p}{2\pi}(x_c + x_c^3 + x_c^5). \tag{9}$$

We provide only the solution under the first-order approximation, since the solutions under the third- and fifth-order approximations containing Jacobi cn functions are too long to be showed,

$$x_c^{(z)} = x_{c0}\cos\left(\sqrt{\frac{p}{\pi}}z\right), \tag{10}$$

where x_{c0} is the normalized input offset. The normalized output coordinate $x_c^{(l)}$, where l is the normalized length of the lead glass, is proportional to x_{c0} when the input light power maintains constant.

Figure 2(a) pictures the oscillation period of the soliton trajectory versus the input offset. The period decreases when the input offset approaches to the boundary. This is understandable, since strong boundary effect accelerates the oscillation of the beam. Figure 2(b) is the beam oscillation at the input offset of $0.4R$. The analytical result under the fifth order approximation is best fit to the numerical result.

Our experimental setup is similar to that in the work of Alfassi *et al.* [6]. The sample is a cylindrical heavily lead-doped glass sample with the radius $R=1.5$ mm and length $L=5$ cm [Fig. 1(a)]. The absorption coefficient $\alpha=0.07\ \mathrm{cm}^{-1}$, the thermo-optical coefficient $\beta=14\times10^{-6}\ \mathrm{K}^{-1}$, the refractive index $n_0=1.9$, and the thermal conductivity $\kappa=0.7\ \mathrm{W/(mK)}$. The 50 μm FWHM light input is produced by a double-frequency YAG laser (Verdi 5) with the wavelength 532 nm. The soliton critical power is measured to be 500 mW, which is in good agreement with the ana-

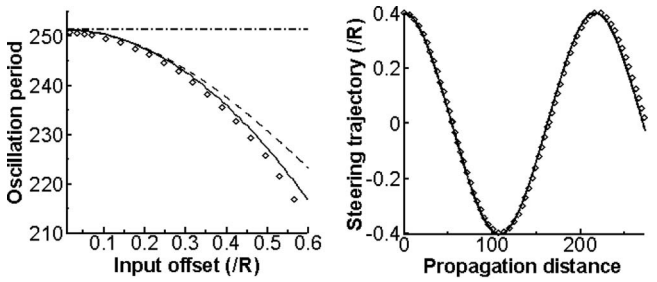

Fig. 2. (a) Oscillation period of the soliton trajectory verses the input offset. The dashed-dotted line, the dashed curve, and the solid curve are the analytical results under the first-order approximation, the third-order approximation, and the fifth-order approximation, respectively. The circles are the numerical results. (b) Beam oscillation at the input offset of $0.4R$ versus the propagation distance. The comparison is between the analytical result under the fifth-order approximation (solid curve) and the numerical result (circles). The oscillation period in Fig. 2(a) and the propagation distance in Fig. 2(b) are normalized by the Rayleigh distance with $w_0 = 1/30R$.

lytical value [19]. The data of the steering experiment are obtained under the higher light power of 700 mW. Figure 3 gives the comparisons between the experimental data and the analytical fitting curves. The first approximation solution is a straight line; it can be fitted to the experimental data only when the input offset is small enough. The higher-order approximation gives the better agreement with the experimental result. It is noticeable that in Fig. 2(a) the oscillation period of the soliton trajectory is far longer than the length of the glass, which is only several times of the Rayleigh distance. Yet, we cannot obtain larger steering output via lengthening the glass, because the absorption will result in the changing of the beam width even the collapse of the soliton.

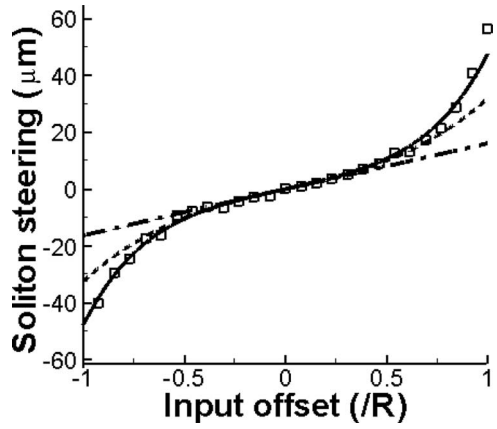

Fig. 3. Net steering relative to the input offset verses the input offset. Squares, experimental result; dashed-dotted curve, first approximation solution $x_{c0}-x_c^{(1)}$; dashed curve, third approximation solution $x_{c0}-x_c^{(3)}$; solid curve, fifth approximation solution $x_{c0}-x_c^{(5)}$.

In conclusion, the soliton propagation in cylindrical lead glass is studied. A method of image beam of light is produced by analogy with the method of images in the electrostatics. The boundary effect on the soliton is treated as the interforce between the soliton beam and the image beam located at the image point. The analytical solution of the soliton trajectory is in good agreement with the experimental results. The method of image beam of light is useful in the treatment of the boundary problems, including the influence of the boundary force on the soliton trajectory and even the interaction between solitons via the boundary effect.

This research was supported by the National Natural Science Foundation of China (NSFC) (grants 10804033 and 10674050) and Program for Innovative Research Team of the Higher Education in Guangdong (grant 06CXTD005).

References

1. A. W. Snyder and D. J. Mitchell, Science **276**, 1538 (1997).
2. C. Rotschild, M. Segev, Z. Y. Xu, Y. V. Kartashov, and L. Torner, Opt. Lett. **31**, 3312 (2006).
3. C. Rotschild, B. Alfassi, O. Cohen, and M. Segev, Nat. Phys. **2**, 769 (2006).
4. B. Alfassi, C. Rotschild, O. Manela, M. Segev, and D. N. Christodoulides, Phys. Rev. Lett. **98**, 213901 (2007).
5. C. Rotschild, O. Cohen, O. Manela, and M. Segev, Phys. Rev. Lett. **95**, 213904 (2005).
6. B. Alfassi, C. Rotschild, O. Manela, and M. Segev, Opt. Lett. **32**, 154 (2007).
7. A. Alberucci, M. Peccianti, and G. Assanto, Opt. Lett. **32**, 2795 (2007).
8. A. Alberucci and G. Assanto, J. Opt. Soc. Am. B **24**, 2314 (2007).
9. M. Peccianti, A. De Rossi, G. Assanto, A. De Luca, C. Umeton, and I. C. Khoo, Appl. Phys. Lett. **77**, 7 (2000).
10. M. Peccianti, K. A. Brzdakiewicz, and G. Assanto, Opt. Lett. **27**, 1460 (2002).
11. C. Conti, M. Peccianti, and G. Assanto, Phys. Rev. Lett. **91**, 073901 (2003).
12. M. Peccianti, C. Conti, G. Assanto, A. De Luca, and C. Umeton, Nature **432**, 733 (2004).
13. Q. Guo, B. Luo, F. H. Yi, S. Chi, and Y. Q. Xie, Phys. Rev. E **69**, 016602 (2004).
14. W. Hu, T. Zhang, Q. Guo, L. Xuan, and S. Lan, Appl. Phys. Lett. **89**, 071111 (2006).
15. Z. P. Dai, Y. Q. Wang, and Q. Guo, Phys. Rev. A **77**, 063834 (2008).
16. D. M. Deng and Q. Guo, Opt. Lett. **32**, 3206 (2007).
17. A. B. Aceves, J. V. Moloney, and A. C. Newell, Phys. Rev. A **39**, 1809 (1989).
18. J. D. Jackson, *Classical Electrodynamics*, 3rd ed. (Wiley, 1999).
19. Y. B. Liang, Y. J. Zheng, P. B. Yang, L. G. Cao, D. Q. Lu, W. Hu, and Q. Guo, Acta Phys. Sin. **57**, 5690 (2008).